International Journal for Modern Trends in Science and Technology
Volume 9, Issue 10, pages 69-83.
ISSN: 2455-3778 online
Available online at: http://www.ijmtst.com/vol9issue10.html
DOI: https://doi.org/10.46501/IJMTST0910009

A Single - Stage Three - Phase Grid Connected PV-UPQC System

Choppakatla Gayathri[1] | P. Buchi Babu[2]

[1]Department of Electrical and Electronic Engineering, G. Narayanamma Institute of Technology & Science, JNTUH, Kukatpally, Hyderabad.
[2]Department of Electrical and Electronic Engineering, G. Narayanamma Institute of Technology & Science, JNTUH, Kukatpally, Hyderabad.

To Cite this Article
Choppakatla Gayathri and P. Buchi Babu. A Single - Stage Three - Phase Grid Connected PV-UPQC System, International Journal for Modern Trends in Science and Technology, 2023, 9(10), pages. 69-83. https://doi.org/10.46501/IJMTST0910009

Article Info
Received: 17 October 2023; Accepted: 28 October 2023; Published: 02 November 2023.

ABSTRACT

This study presents a novel approach to enhance grid power quality by integrating a Unified Power Quality Conditioner (UPQC) with a hybrid energy storage system consisting of solar panels and battery super capacitors. The increasing integration of renewable energy sources in the grid has led to challenges in maintaining power quality due to their intermittent nature. The UPQC is a versatile solution for mitigating power quality issues, including voltage sags, voltage swells, and harmonic distortions. In this research, the UPQC is synergistically combined with a hybrid energy storage system to create a comprehensive power quality enhancement solution. The solar panels contribute clean energy generation, while the battery super capacitors offer rapid energy injection and absorption capabilities. This integrated system not only improves power quality by compensating for grid disturbances but also facilitates the effective utilization of surplus energy. The control strategy for the proposed system is designed to ensure seamless coordination between the UPQC and the energy storage components, optimizing their performance for various power quality events. Simulation studies conducted on a representative grid system demonstrate the effectiveness of the proposed integrated solution in mitigating power quality issues and enhancing grid stability. The results showcase a significant reduction in voltage deviations and harmonic distortions, thereby underlining the system's potential to revolutionize grid-connected power systems.

KEYWORDS: Maximum power point tracking (MPPT), power quality, shunt compensator, series compensator, solar photovoltaic (PV), Battery energy storage system (BATTERY AND SUPER CAPACITOR STORAGE SYSTEM), Super-Capacitor, unified power quality conditioner (UPQC).

1. INTRODUCTION

Energy is essential for the survival of all living beings. Electricity is a significant kind of energy among the numerous available. It ensures life's flexibility, and its need is rising rapidly. Rising energy demand in recent years has led to issues with power quality. The increase in need is being fueled by demographic shifts and technological progress. Because they depend on

nonrenewable conventional energy sources, our present practices cannot keep up with the increase in demand. Conventional energy production makes extensive use of fossil fuels including oil, coal, crude oil, and natural gas. Therefore, we need to integrate nonconventional energy sources like solar, wind, water, biogas, tidal, geothermal, etc., with the conventional method to meet future demand. Solar power is rapidly replacing other renewable energy sources as the most popular option because of its numerous advantages, such as cheaper energy production costs and zero greenhouse gas emissions. Power quality and reliability have deteriorated as a result of increasing consumer demand for electricity, the prevalence of nonlinear loads, and the advent of renewable energy sources like Photovoltaic (PV) and wind power [1, 2]. Due to the widespread use of power electronics and other nonlinear devices, electric power networks produce excessive quantities of harmonics and reactive current. The impedance of the circuit causes distortion of the grid voltage and a slowing of the power consumption rate. In addition, the widespread grid voltage fluctuation, three-phase imbalance, and short outages will have a significant influence on the performance of currently running industrial equipment, leading to massive economic losses. One of the most basic and critical issues in power quality is, therefore, maintaining a steady and pure sine wave for both the grid current and the load voltage. Power electronic equipment including as passive LC filters, Static var Generation, active power filters, and dynamic voltage restorers are often utilized to address modern-day power quality issues. However, its simplex nature restricts their use to a limited set of power quality problems. Because of its many useful functions, UPQC may be a good choice for improving power dependability. However, the Unified Power Quality Conditioner's (UPQC) potential to enhance power quality and correct for sag/swell voltages in distribution networks has piqued the interest of many academics. While the UPQC was first developed for use with shunt and series power converters connected by DC-link [3], it has since attracted attention from a wide variety of disciplines and been applied in a wide variety of ways. Sags and surges are examples of complicated power quality situations [4], in which many power quality concerns have joined together to generate a single interruption. Voltage harmonics, swells, and sags may all cause sensitive loads and other pieces of equipment to trip, which can have serious consequences for manufacturing plants. These misfortunes are all too common in the sector and can lead to substantial monetary losses. Industrial customers have started installing devices from the series APFs to mitigate grid interruptions [5-10]. Shunt active power filters (APFs) are used to lessen the impact of harmonics generation and sensitive load in modern power plants due to the prevalence of power electronics [11-14]. This has resulted in the development of a new norm that satisfies the needs of the utility and its clientele. Customers' loads don't alter the utility's supply unnecessarily, and the utility's critical components are shielded from voltage fluctuations, thus everyone wins [15]. To control both the load voltage and the grid current, the UPQC model is constructed by connecting series and shunt APF compensators in a back-to-back arrangement [16]. Academics' interest in UPQC [17-20] has been spurred by the rising prevalence of microgrids and decentralised power plants. The use of fossil fuels, which contribute to and are itself a cause of global warming, has come under increased scrutiny, and so has the pursuit of alternative, renewable power sources. Improved renewable energy systems that can continue operating in the event of a grid outage are urgently needed to meet this demand. [21] successfully exhibited a fuel cell (FC) coupled with UPQC to offer real power supply during voltage breakdown, hence mitigating PQ issues on the grid side. Despite this, their studies have not advocated for decarburization of the grid-connected system or stressed the combination of renewable energy supplies with UPQC. Power quality issues and renewable energy supply were combined in [22, 23] with the proposal of a PV integrated with UPQC. Prolonged interruption and considerable power sag, however, were overlooked. Long-term load support was also addressed by the dynamic voltage restorer (DVR) in combination with a superconducting magnetic energy storage system (SMES) [24]. Modern harmonics, on the other hand, were disregarded. The PV-UPQC may be connected to a variety of energy storage devices, including batteries and super capacitors, to provide uninterrupted power delivery to the load. UPQC's battery and super capacitor storage solution becomes essential when applied to critical loads like semiconductor manufacturers, hospitals, and other

establishments that need continuous access to clean, dependable power. As a result, the study recommends a battery and supercapacitor-based energy storage system to back up the UPQC. A single-stage DC-DC buck-boost converter [25, [26]] connects the PV to the DC-link and the battery and super capacitor storage system. However, when the PV system is unable to do so, like during a protracted voltage outage, the battery and super capacitor storage system kicks in to provide the load with active power. Researchers try to construct the algorithm in [21] and [27-29] for controlling the voltage across the DC-link capacitor. However, UPQC controllers continue to increase in complexity and computational burden. Using an external support system, such as a PV-battery and super capacitor storage system, may reduce the load on a UPQC's DC-link capacitor. Since the PV array is wired into the UPQC DC-link, designers needed to ensure that the MPP voltage matched the DC-link's reference voltage. Under normal circumstances, the PV array's rating provides more than enough active power to run the load, feed the grid, and charge the BESS. When the DC-link load requires more power than the PV array can provide, the battery and super capacitor storage system kicks in to restore the DC-link voltage. In addition, the battery and super capacitor storage system will provide for the whole load need even if the PV array is not producing any electricity. PV-UPQC regulation relies heavily on the production of a reference signal. Both time-domain and frequency-domain methods exist for generating reference signals [30]. Due to the minimal processing needs, time-domain methods are often employed for real-time implementation. There are several well-known methods to this problem [31], including the p-q theory of instantaneous reactive power, the d-q theory of synchronous reference frames, and the symmetrized component theory. The most significant barrier to using a solution predicated on the synchronous reference frame theory is the presence of a double harmonic component in the d-axis current under a load unbalanced situation. Therefore, low-pass filters with an extremely low cut off frequency are often used to eliminate the double harmonic component. The result is poor dynamic performance [32]. The d-axis current is separated from the basic load active current by use of a moving average filter (MAF). By doing so, we may increase attenuation while minimising the load on the controller's bandwidth [33]. Recent applications of MAF include improving the efficiency of dc-link controllers [35] and grid synchronisation through phase-locked loop (PLL) [34]. Our study details the planning, implementation, and analysis of a three-stage PV-UPQC system. Dynamic performance is enhanced by active current extraction from the load when a MAF-based d-q theory-based control is used.

2. POWER QUALITY ISSUES

The Power System is experiencing severe issues with power quality (PQ). Because poor power quality causes companies to lose money and experience equipment failure. Power quality issues manifest themselves in a variety of ways, including voltage dips, short interruptions, extended interruptions, voltage spikes, harmonic distortion, fluctuations, flashes, and swells. It is challenging to incorporate wind into the grid since wind flow changes and we need to maintain a steady power quality (PQ) without compromising system efficiency. WECS PQ may be enhanced with the use of reactive power compensation methods, UPQC controllers, and fact devices.

A. Voltage variation/Voltage flickering

The system's P and Q powers are directly proportional to the fluctuations in voltage. Changes in solar irradiance are the primary cause of voltage shifts. Cloud cover, shadowing, and diurnal changes in sunshine have long been obstacles to the widespread use of solar energy. When solar panels are linked to the power grid, the voltage at that point might be affected by these variations. Voltage flickering is particularly concerning since its rapid and repetitive voltage changes may disrupt sensitive loads and lower the efficiency of connected devices. Voltage sags or voltage dips are temporary reductions in voltage that occur at the system power frequency and last for half a cycle. Several things may cause voltage dips, such as a sudden change in demand, the shutting down of turbines, or difficulties with the power grid's transmission or distribution networks. Unregulated use of transformers, issues in the power distribution system, and the sudden addition or removal of significant loads are all potential causes of voltage spikes. Voltage fluctuations may cause all sorts of problems, including the destruction of

expensive machinery, the failure of relays and circuit breakers, the flickering of lights and screens, and so on. Voltage flickering is a common problem with wind power systems that are linked to the grid because of the constant power fluctuations, switching activities, and poor performance of sensitive electronic components.

B. Harmonics

Sinusoidal waves with frequencies that are multiples of the fundamental frequency may be found in these currents or voltages. Non-linear loads, current and voltage waveform disruption, frequency mismatch between system and equipment, etc. all play a role in this phenomena, as does the functioning of power electronics converters. Negative consequences of harmonics include damage to protective equipment, faulty transformer operation, increased system losses, reduced system efficiency, motor and capacitor bank overheating, and so on.

C. Transients

Internal faults and external faults are the two most common sources of transients. Equipment activation or deactivation, such as circuit breakers, relays, power electronics, etc., is an example of an internal malfunction. A surge in the current flowing through the system may be caused by an external problem, such as a lightning strike. A lightning arrestor should be fitted as a precaution against lightning strikes before any electrical equipment.

3. System Configuration and Design

Fig. 1 depicts the PV-ESS-UPQC in its physical form. The PV-BESS-UPQC model is compatible with the three-phase system. A series and shunt APF compensator, as well as a DC-link split capacitor, make up the PV-ESS-UPQC. The DC-link is linked in parallel with the PV array and the batteries. The PV is connected to the DC-link through a boost converter. The DC-link is connected to the BESS through a buck-boost converter. The supply voltage's spikes, dips, interruptions, and harmonics are all neutralised by the series compensator, which acts as a regulated voltage source. Shunt compensators are used to reduce load current harmonics. Connecting the series and shunt APF compensators calls for the use of inductors. Since harmonics are created by the converter's switching motion, a ripple filter is utilised to eliminate them. In order to inject power into the grid, the series compensator makes use of a series injection transformer. A three-phase non-linear load is employed in this investigation. Accurate measurements of the PV array, split capacitor, reference voltage of DC-link, etc., are required before a PV-ESS- UPQC can be designed. The shunt compensator is built to regulate the maximum power output of the PV array in addition to reducing current harmonics. Since the PV array is wired into the UPQC DC-link, designers needed to ensure that the MPP voltage matched the DC-link's reference voltage. Power generated by the PV array is sent into the grid and used to charge the ESS (energy storage system) under normal circumstances. The BESS kicks in to supplement the DC-link load when the energy supplied by the PV arrays is inadequate. When the PV array is not producing any electricity, the ESS will take over and provide all of the necessary power.

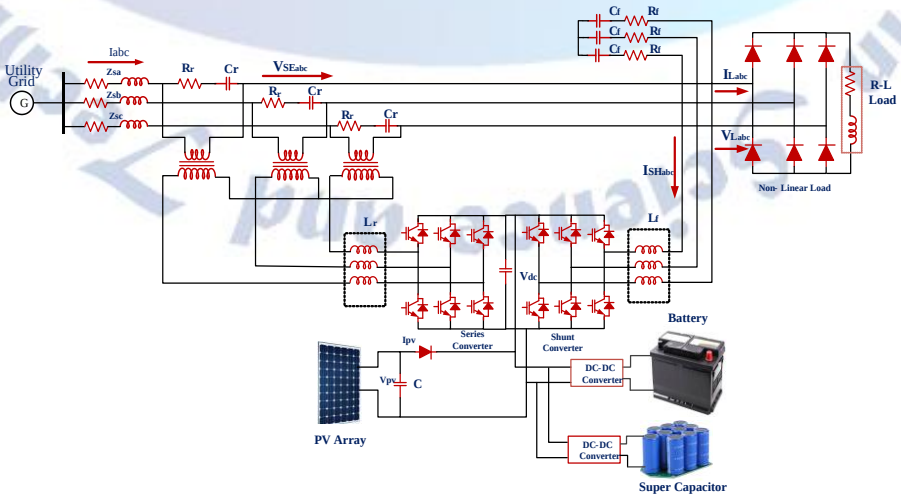

FIGURE 1. UPQC system configuration.

4. System Analysis

D. Modeling of Solar PV system

Figure 2 illustrates the equation for the voltage/current characteristic of a solar cell with a light source and a diode. Connecting solar cells in series and parallel inside a module allows the output of a solar panel to be modified. The quantity of solar energy (in photons) entering a solar cell is proportional to the photocurrent I_{Ph} flowing

through the cell.

The current drawn by a solar panel may be determined using Kirchoff's current law (KCL), as seen in Fig.

$$I_{PV} = I_{Ph} - I_D - I_{Rsh} \quad (1)$$

Environment variables such as irradiance and temperature form the basis of I_{Ph}. Here's how you figure out your I_{Ph}:

$$I_{Ph} = \left(I_{sc} + \alpha\left(T_C - T_{ref}\right)\right)\frac{\lambda}{\lambda_{ref}} \quad (2)$$

I_D is an exponential function representing the diode current.

$$I_D = I_s\left[\exp\left(\frac{q\left(V_{PV}+R_sI_{PV}\right)}{AkT_C}\right) - 1\right] \quad (3)$$

Saturation current in a solar cell shows the effect of temperature and an exponential function. I_s may be calculated as

$$I_s = I_{Rs}\left(\frac{T_C}{T_{ref}}\right)^3 \exp\left[\frac{qE_g\left(\frac{1}{T_{ref}}-\frac{1}{TC}\right)}{KA}\right] \quad (4)$$

Saturation current in the opposite direction is represented by the exponential function I_{RS}.

$$I_{Rs} = \frac{I_{SC}}{\exp\left(\frac{qV_{OC}}{AkT_C}\right)-1} \quad (5)$$

As can be seen in Fig. 2, Kirchoff's voltage law is used to determine the current via the shunt resistor, represented by I_{RSh}. Following is the equation for I_{RSh}:

$$I_{Rsh} = \frac{V_{PV}+R_sI_{PV}}{R_{sh}} \quad (6)$$

To get I_{PV} defining feature, we can rewrite Eq. 1 as follows.

$$I_{PV} = I_{Ph} - I_s\left[\exp\left(\frac{q\left(V_{PV}+R_sI_{PV}\right)}{AkT_C}\right) - 1\right] - \frac{V_{PV}+R_sI_{PV}}{R_{sh}} \quad (7)$$

$$I_{Pv} = N_PI_{Ph} - N_pI_s\left[\exp\left(\frac{q\left(\frac{V_{PV}}{Ns}+\frac{R_SI_{PV}}{N_P}\right)}{AkT_C}\right) - 1\right] - \frac{\frac{N_PV_{PV}}{N_S}+R_sI_{PV}}{R_{Sh}} \quad (8)$$

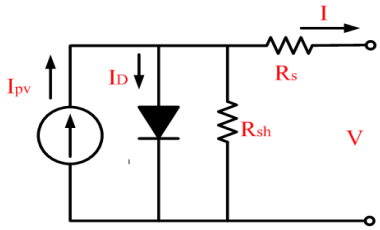

Fig 2. A PV cell's equivalent circuit

where,

I_{PV} : The output current of solar panel (A)
V_{PV} : The output voltage of solar panel (V)
I_{sc} : Short circuit current (A)
V_{oc} : Open circuit voltage (V)
α : Temperature coefficient $(V/°C)$
T_c : Solar panel temperature (K)
T_{ref} : Solar panel reference temperature (K)
λ : Irradiance $(W/m2)$
λ_{ref} : Reference Irradiance $(W/m2)$
K : Boltzman's contant (1.38 × 10−23)
A : Ideality factor
q : Elementary charge (1.6 × 10−19 C)
E_g : Band gap energy of the semiconductor (eV)

E. Battery System Model

a. ESS Batteries

Li-ion batteries are employed for the ESS in this study. Li-ion batteries are often used in energy storage devices. For lack of better options, Li-ion batteries have been settled upon as the ESS for CS due to its high efficiency (85%-95%), high energy density (1,000-2,000 mAh/kg), and many re-use potentials. The method proved effective in controlled laboratory settings. The ESS's batteries were simulated using Simulink battery model, with values taken from the corresponding product datasheets. This kind has a voltage regulator and a series resistance. The battery voltage, V_{bat} (see Eq. (11), which is derived from Eq. (9), is the difference between the open-circuit battery voltage and the internal battery resistance, R_{int}. Knowing the battery type is crucial for calculating E_{bat} and the value of R_{int}.

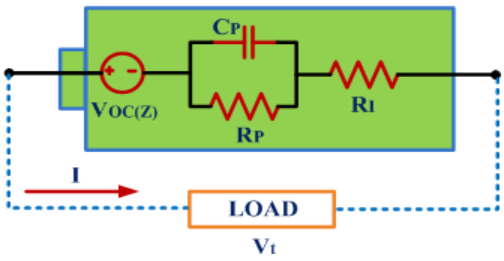

Fig. 3. Model of a Circuit for a Lithium-Ion Battery

State of Charge Equation:

$$z(t) = z(0) - \frac{\int_0^t I(\tau)\, d\tau}{Q_{max}} \quad (9)$$

$$z(t) = -\frac{I(t)}{Q_{max}} \quad (10)$$

Model Equation:

$$V_P(t) = -\frac{V_P(t)}{R_P C_P} + \frac{I(t)}{C_P} \quad (11)$$

$$(t) = V_{oc}(z) - V_P - I(t) \cdot R_I \quad (12)$$

b. Li-ion Battery Circuit Model

Open-circuit voltage (Voc) at time (t) equals charge (Q). Polarization RI Voltage Number Terminal voltage (V_t), current (A), and internal resistance are all shown. In the Li-ion Battery Equivalent Circuit Model, the cell's usable voltage is reduced due to polarization and the internal IR drop. Open circuit voltage and maximum potential energy can only be achieved by running cells at extremely low operating currents. When polarization and IR drop are minimal, charging and overcharging currents perform well. Changing the open circuit voltage and polarization of a cell causes an increase in equivalent series resistance (ESR) and I_R drop, reducing the battery's energy density.

$$V_t(t) = V_{oc}(z) - V_P - I(t) \cdot R_I \quad (13)$$

Simply counting coulombs (Eq. (14), where Q is the battery's maximum capacity) yields the battery's state of charge.

$$SOC(\%) = SOC_0(\%) - 100\left(\frac{\int I_{bat} \cdot dt}{Q}\right) \quad (14)$$

The kinetic behavior of this battery model was demonstrated to be similar to the experimental behavior for states of charge (SOC) between 100% and 20% during charging and discharging. Our findings indicate that the battery may be used securely at a state of charge (SOC) of 20% to 100%, which means that severe discharge is not required. Coulomb counting is often employed for SOC determination since it requires less computer resources. The experiment's Li-ion battery has fewer and milder side effects compared to regular batteries. The mistake in the present integration just becomes worse as time goes on, which is a major problem with this strategy. This method's accuracy depends on the test duration and capacity knowledge, as well as the present accuracy of the sensor. Errors in the current measures utilised in this method compound up over time and have a significant impact on the projected outcomes. Since only simulations are shown, it is assumed that the current measurement and, by extension, SOC are correct.

c. BESS converter configuration

The voltage in a hybrid system is optimised in a way that minimises energy waste without sacrificing performance. The voltage feeder of the hybrid system may be connected to renewable energy sources including hydro, wind, and solar. As can be seen in Figure 4, the ESSs are linked to the DC bus through a bidirectional DC converter. DC-DC converter systems are often used as an interface between the DC bus and the energy storage device to stabilise the DC voltage. For optimal system performance, it is essential that bidirectional converters provide many modes of operation.

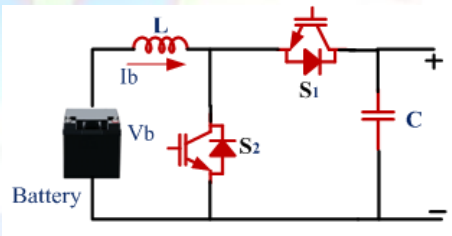

Fig 4. Battery storage system with controller

Mode 1: When the battery is being charged, the converter switches into buck mode via switch b1 and diode b2.

Mode 2: During power outages, the converter operates in boost mode to satisfy the DC bus requirement, and switch b2 and diode D1conduct to allow the battery power to serve the load.

Mode 3: Battery power is kept in float mode (trickle charging mode) while it is not being used to keep the voltage and state of charge steady.

F. Super Capacitor Modeling

A super capacitor has two electrodes separated by an

ion-permeable separator to prevent electrical current from flowing directly between them. Fast charging and discharging rates, low internal resistance, and a long cycle life give these batteries their distinctive high power density and efficiency. Many alternative circuit models including super capacitors have already been published. Capacitors may be used to store electricity. Since there are no chemical or phase changes during the process, the discharge-charge cycle may be repeated indefinitely. Electrochemical capacitors (ECs) are marketed under a variety of names owing to their very high capacitance values, including super capacitors, ultra-capacitors, and electric double layer capacitors (EDLCs). Commercially available capacitors in a common case size have recharge capacitance values up to 400 Farads. Modern super capacitors' capacitance density is second only to that of batteries, making them perfect for many uses that formerly needed batteries but now can make do with much smaller devices. For large-scale energy storage applications, a super capacitor is preferable than a battery due to its better efficiency and higher cost, among other benefits.

a. Design of super capacitor energy storage system

Before building a Super capacitor energy storage system, it's important to calculate the overall capacitance of the system. V_{Cell} is what decides how much power a Super capacitor bank can store electrically. If the super capacitor's rated voltage is V_{Cell}.

$$V_{scmax} = n_s * V_{Cell} \quad (15)$$

When n s super capacitor cells are linked together in series, a string is created. R_{Cell} also provides the series ESR of string, which is analogous to R_{Cell}.

$$R_s = n_s{}^* R_{Cell} \quad (16)$$

The series capacitance (C_s) of a string of n_s super capacitor cells is

$$C_s = \frac{C_{Cell}}{n_s} \quad (17)$$

The formula gives I_{scMax} as the maximum allowable current across the bank of super capacitors.

$$I_{scmax} = \frac{I_{scmax}}{I_{Cell}} \quad (18)$$

Each series string (I_{Cell}) of n_s series super capacitor cells has a current lower than I_{scMax}, where P_{sc} is the rated power of the super capacitor bank. It is possible to calculate the number of series strings in parallel using I_{scMax} and I_{Cell}.

$$n_p = \frac{I_{scmax}}{I_{Cell}} \quad (19)$$

Equivalent super capacitance due to n_p resistance of each C_s

$$C_{sc} = n_p{}^* C_s \quad (20)$$

Equivalent series resistance (R_{sc}) due to n_p of each R_s

$$R_{sc} = \frac{R_s}{n_p} \quad (21)$$

Energy of super capacitor (E_{sc}) with the help of V_{sc} and C_{sc}

$$E_{sc} = \frac{1}{2} * C_{sC} * V_{sc}^2 \quad (22)$$

The nominal voltage (highest voltage) V_{scnom} and the minimum voltage V_{scmin} are used to get the super capacitor capacitance c_{sc}.

$$C_{sc} = \frac{2 * P_{sc} * t_d}{(V_{scnom} - V_{scmin})^2} \quad (23)$$

Where $E_{sc} = P_{sc} * t_d$

b. RC Circuit Model

The ultra capacitor may be modeled using a simple RC circuit, as seen in Fig. 5. It consists of the three components necessary for a functional circuit: The ultra capacitor loses energy when charging and discharging owing to three factors: a capacitance c_{sc}, a series resistor R_s (also known as the equivalent series resistor; ESR); and a parallel resistor R_P (also known as the leakage resistance). This model has been constructed in several studies and has been corroborated by data. The current state of affairs might be stated as

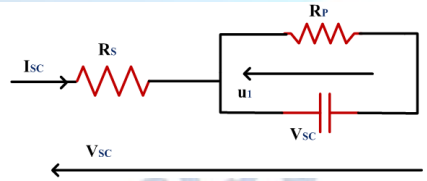

Fig.5. Super capacitor Equivalent Model

$$\frac{du_1(t)}{dt} = \frac{-u_1(t)}{R_P C_{sC}} + \frac{I_{sc}}{c_{sc}} \quad (24)$$

$$V_{sc}(t) = R_s I_{sC} + u_1(t) \quad (25)$$

c. Bi-directional dc-dc super capacitor converter

Since the super capacitor is unable to directly inject the power, a converter must be used to link the DC connection between the super capacitor and the hydro generator. An inductor is connected in series with a super capacitor to smooth out voltage and current spikes. In Fig. 6, we can see the whole SCESS circuit design. Two IGBT switches are used in this case. When two IGBTs are connected in series, the result is buck mode switching, but when two are connected in shunt, the result is boost mode switching. There are four different ways to use this circuit. The super capacitor is charged when the DC link voltage is higher than the reference voltage (buck mode), and discharged when the DC link voltage drops below the reference voltage (boost mode).

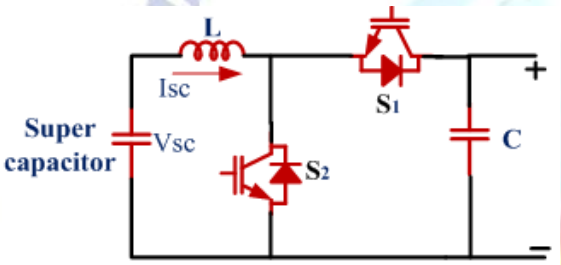

Fig 6. Super capacitor energy storage system with controller

Mode 1: During super capacitor charging, the converter is in buck mode and the switch S1 and diode S2 are active.

Mode 2: Switch S2 and diode D1 conduct, and the converter enters boost mode to provide the DC bus with the current needed to drive the load when the power grid goes down.

Mode 3: The super capacitor is kept at a stable voltage and state of charge (SOC) by switching to float mode (trickle charging mode) while it is not being used.

5. CONTROL OF UPQC

The shunt compensator and the series compensator are the two most important parts of a PV-UPQC system. Harmonics in the load current and reactive power are two examples of power quality issues that may be mitigated with the use of a shunt compensator. In PV-UPQC, the shunt compensator is also in charge of feeding energy from the PV system into the grid. The shunt compensator uses a maximum power point tracking (MPPT) algorithm to draw power from the PV-array. By injecting the correct voltage in phase with the grid voltage, the series compensator safeguards the load against power quality issues on the grid side, such as voltage sags and surges.

G. Control of Shunt Compensator

The shunt compensator keeps the solar PV-array at maximum efficiency so that all of the power it can produce is used. In PV-UPQC, the dc-link reference voltage is produced via the MPPT algorithm. Two of the most popular MPPT algorithms are P&O and incremental conductance. In this piece, the P&O approach is used to execute MPPT. A proportional integral (PI)-controller is used to keep the dc-link voltage steady at the preset level. A shunt compensator works by switching the active fundamental component of the load current. Here, the SRF technique is used to regulate the shunt compensator and separate the primary active component of the load current. Figure 7 depicts the control layout for the shunt compensator. The load currents are transformed from the d domain to the q zero domain using the PLL's phase and frequency information. The PCC supplies juice to the PLL. In the abc reference frame, the dc component ($I_{L\,dlf}$) is the basic component, and it is generated from the d-component of the load current ($I_{L\,d}$). A mass airflow sensor (MAF) is utilised to isolate the dc component without compromising the vehicle's dynamic performance. This is the transfer function of MAF:

$$\mathrm{MAF(s)} = \frac{1-e^{-T_w s}}{T_w s} \qquad (26)$$

where Tw is the MAF's window size. Tw is always set to half the period of the fundamental since the double harmonic component of the d-axis current is the lowest harmonic. Zero gain is achieved in the MAF when the window length is an integer multiple of the window size. To represent the PV array's portion of the comparable current, we write

$$I_{PVg} = \frac{2}{3}\frac{P_{PV}}{V_s} \qquad (27)$$

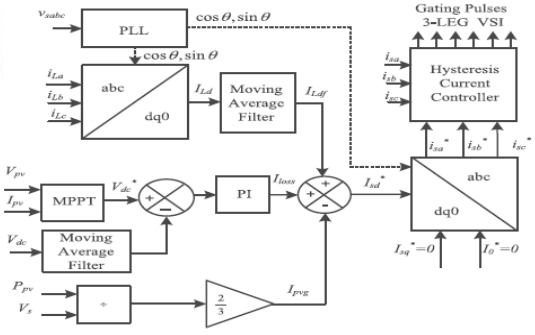

Fig. 7. Shunt compensator control architecture.

Power from the PV array, Ppv, multiplied by PCC voltage, Vs. The d-axis reference grid current is as follows:

$$I_{sd}^{*} = I_{L\,dlf} + I_{Loss} + I_{PVg} \qquad (28)$$

The Isd currents are derived from the abc domain's reference grid currents. The shunt converter's gating pulses in a hysteresis current controller are derived from a comparison of the reference grid currents and the measured grid currents

H. Control of a Series Compensator

Predictive compensation, in-phase compensation, and energy-optimal compensation make up the series compensator's control strategy. The compensation methods used by a series compensator's administrators are described in detail by the authors of [37] and [38]. The series compensator reduces the required injection voltage by coordinating the power injection with the grid voltage. The series compensator's control architecture is shown in Fig. 8. The phase-locked loop (PLL) is utilised to isolate the PCC voltage's fundamental component, which is subsequently used as the d-q-0 domain's reference axis. PLL is used to establish the phase and frequency of the PCC voltage, which is then applied to the reference load to produce the output voltage. The voltages at the power converter choke (PCC) and the loads are transformed from one domain to another, from d to q to 0. The peak load reference voltage is the d-axis value that must be in phase with the voltage from the PCC. Constant zero focus on the q-axis. The series compensator uses a reference voltage calculated by subtracting the voltage from the load reference. The voltages at the series compensators are the load voltage minus the PCC voltage. The PI controller receives the voltage difference between the reference and series compensator outputs so that it can generate accurate reference signals. Gating signals for the series compensator are generated by sending these signals via a pulse-width modulation (PWM) voltage controller after being translated to the abc domain.

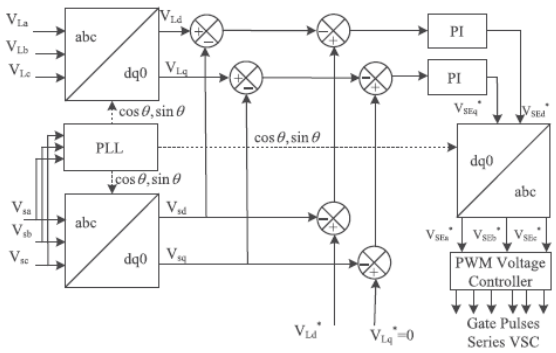

Fig.8. Control structure of a series compensator.

I. Control of a Battery and Super capacitor

Use Figure 9 depicts the battery and super capacitor charging and discharging using a bidirectional buck/boost DC-DC converter control. The outer proportional-integral (PI) controller of the bidirectional buck or bidirectional DC-DC boost converter control regulates the DC link voltage for both the battery and the supercapacitor. Moreover, as shown in Fig. 9, the output of the outer PI controller is the reference battery and supercapacitor current. The inner PI controller is used to monitor the current of the reference battery and supercapacitor. In addition, the duty ratio of the bidirectional buck/boost DC-DC converter is the output of the inner PI controller. The reference battery and supercapacitor current is derived from Figure 9. Refer to DC link voltage and DC link voltage sensed, respectively. Represent the integral and proportional constants of the outer PI controller. In addition, the duty ratio of the bidirectional DC-DC converter is computed and then applied to a PWM generator to generate pulses for the switches of the bidirectional buck or boost converter.

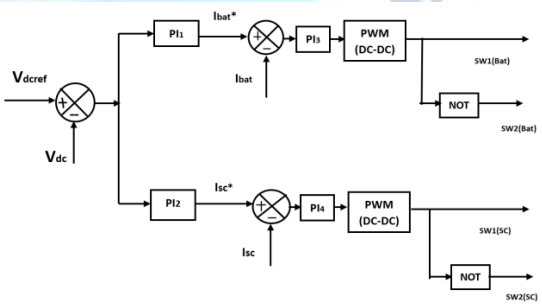

Fig.9. Energy Management Control Strategy for Battery-Supercapacitor Energy Storage System

The duty ratio of the bidirectional DC-DC converter is essential for determining the direction of the power transfer and controlling the output voltage. By modifying the duty ratio, the converter can transfer

energy between the battery and supercapacitor in an efficient manner, ensuring optimal performance and energy management. In addition, the PWM generator plays a crucial role in generating precise pulses for regulating the converter's switches, thereby facilitating a seamless power transfer and minimizing the losses.

6. SIMULATION STUDIES

We use MATLAB-Simulink to model the PV-UPQC system and examine its steady-state and transient behavior. A R-L load in a three-phase diode bridge rectifier serves as the nonlinear load. For this simulation, we chose a solution with a step size of (1e-6) s. The technology is used in a dynamic setting, where factors like PCC voltage and PV irradiance are subject to change.

J. Performance of PV-UPQC at PCC Voltage Fluctuations

Figure 10 depicts PV-UPQC's dynamic performance in the presence of PCC voltage sags/swells. The value of G is kept constant at 1000 W/m2. In addition to the grid current (iS), the signals comprise the current through the load (iLa, iLb, iLc), the current via the shunt compensator (iSHa, iSHb, iSHc), and the power output of the solar PV array (Ppv). In the first quarter of a second, the voltage drops by 0.3 p.u., and in the second quarter, it rises by the same amount. The series compensator injects a voltage vSE that is antiphase to the grid voltage disturbance, keeping the load voltage at its nominal value.

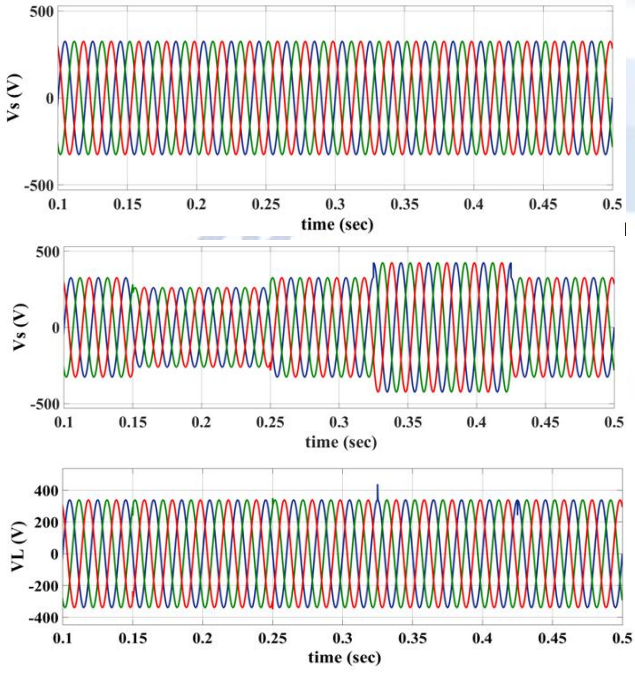

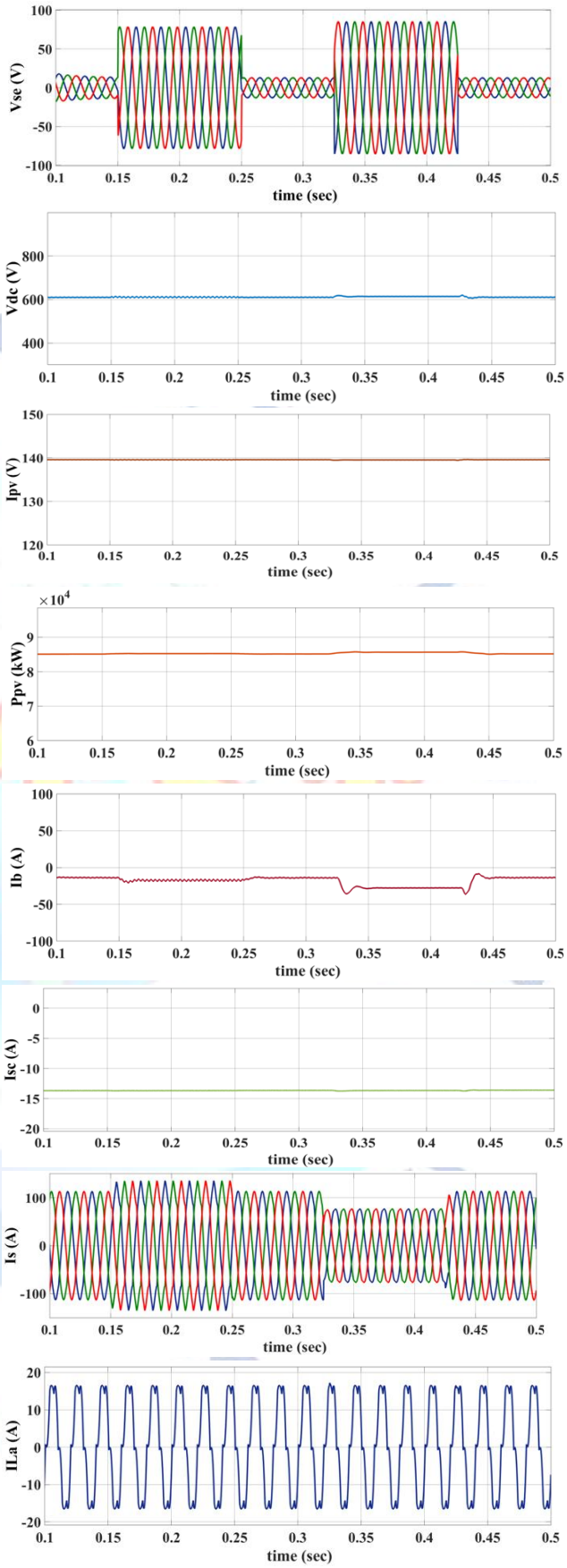

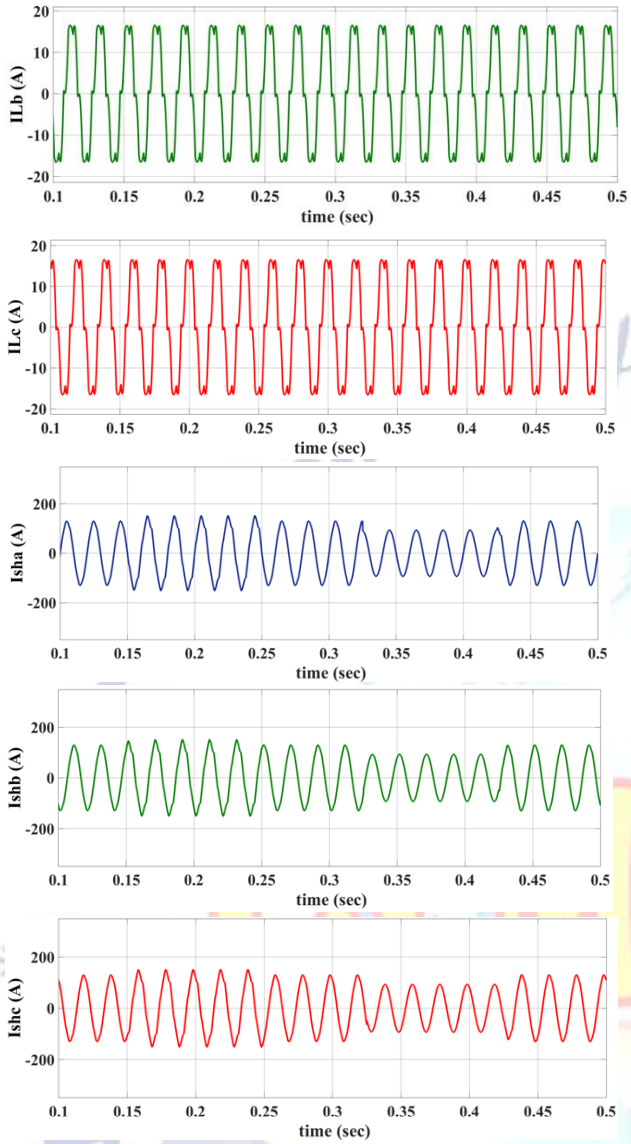

Fig. 10. Performance of PV-UPQC under voltage sag and swell conditions.

K. Performance of PV-UPQC at Load Unbalancing Condition

The dynamic performance of PV-UPQC under an unbalanced load state is shown in Figure 11. Phase "a" of the load is turned off at t = 0.25 s. The grid current is sinusoidal, and the power factor is 1. As the effective load decreases, the grid current increases. The dc-link voltage is likewise consistent, staying within a narrow range of 600 V.

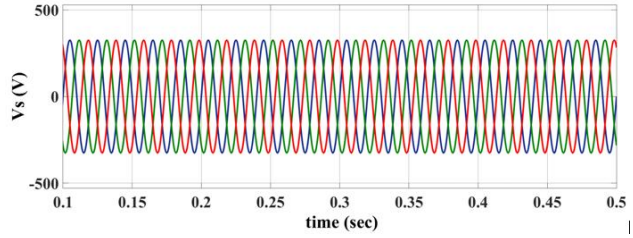

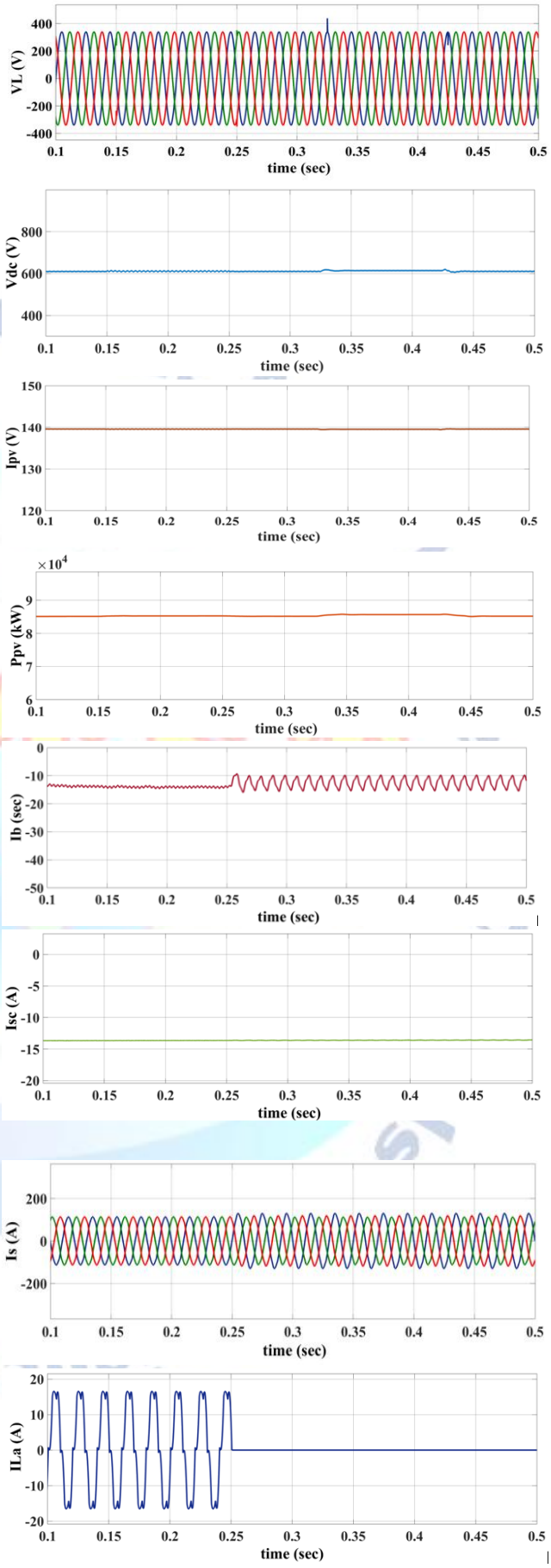

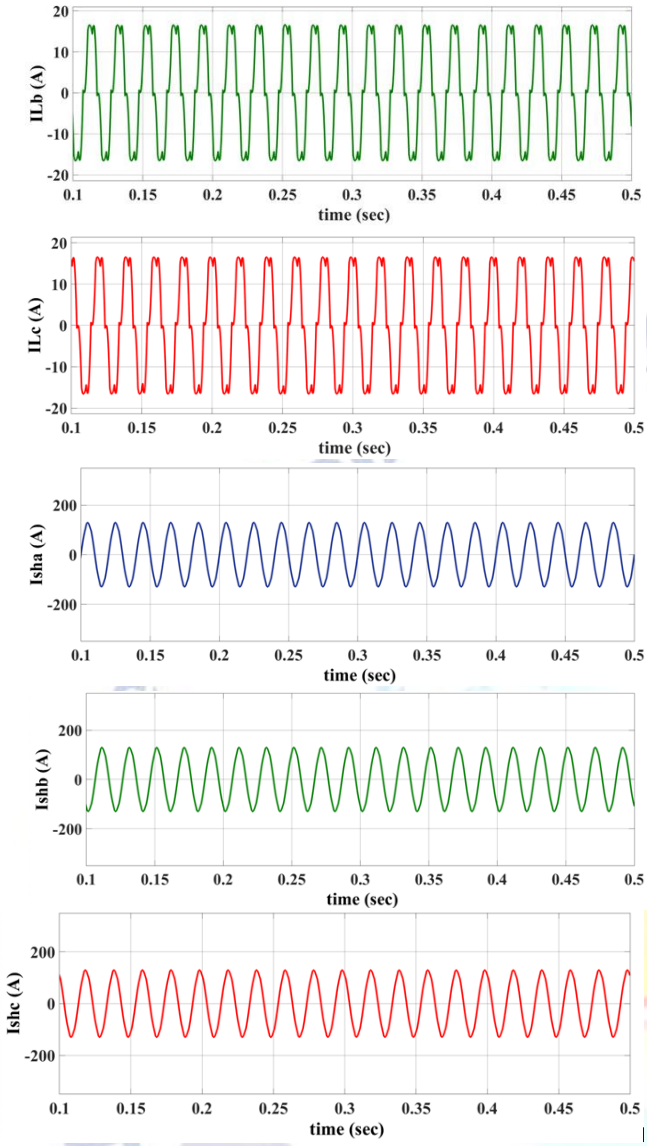

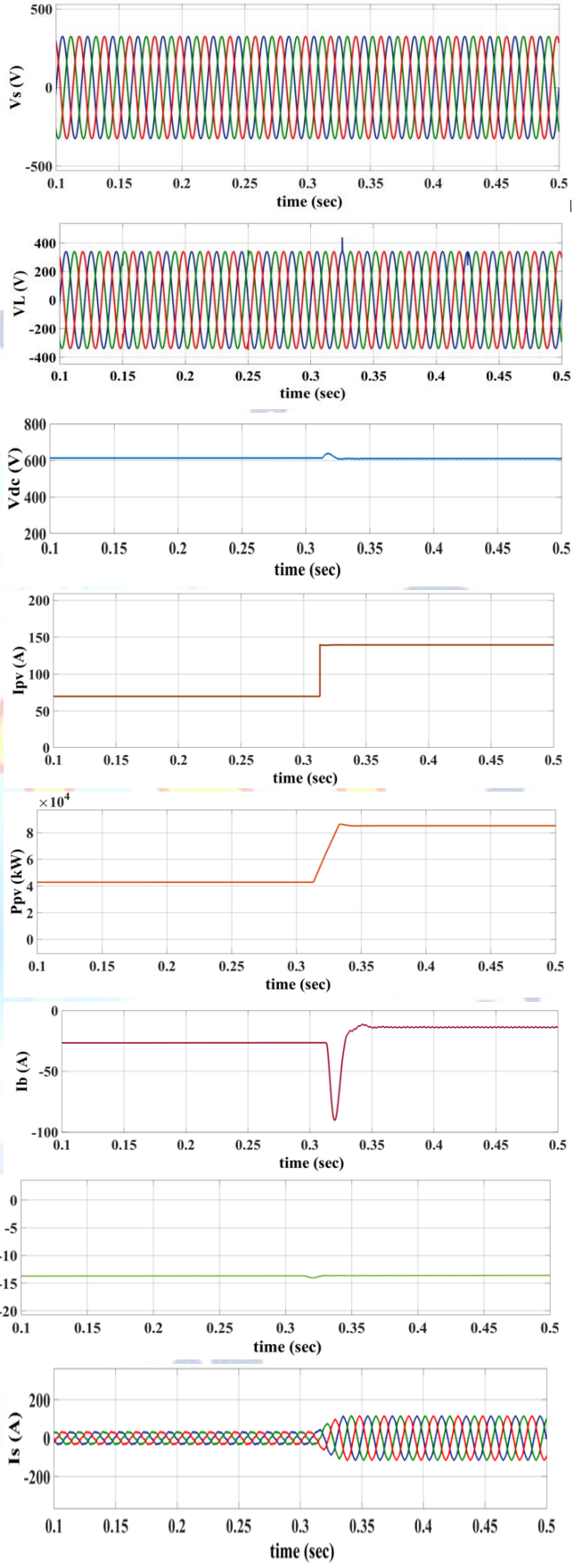

Fig.11. Performance PV-UPQC during load unbalance condition.

L. Performance of PV-UPQC under Varying Irradiation

Figure 12 displays the dynamic performance of PV-UPQC in response to variable solar irradiation. In only 0.315 seconds, the sun's rays go from illuminating at a rate of 500 W/m2 to a whopping 1000 W/m2. It has been shown that as irradiance rises, so does the output of photovoltaic (PV) arrays and, therefore, grid current. In addition to smoothing out harmonics in the load current, the shunt compensator follows maximum power point tracking. Load current and grid current are depicted in Fig. 13, as are the harmonic spectra and total harmonic distortion (THD). IEEE- 519 requirements are met with a total harmonic distortion (THD) reading of 16.96% for the load current and 1.97% for the grid current.

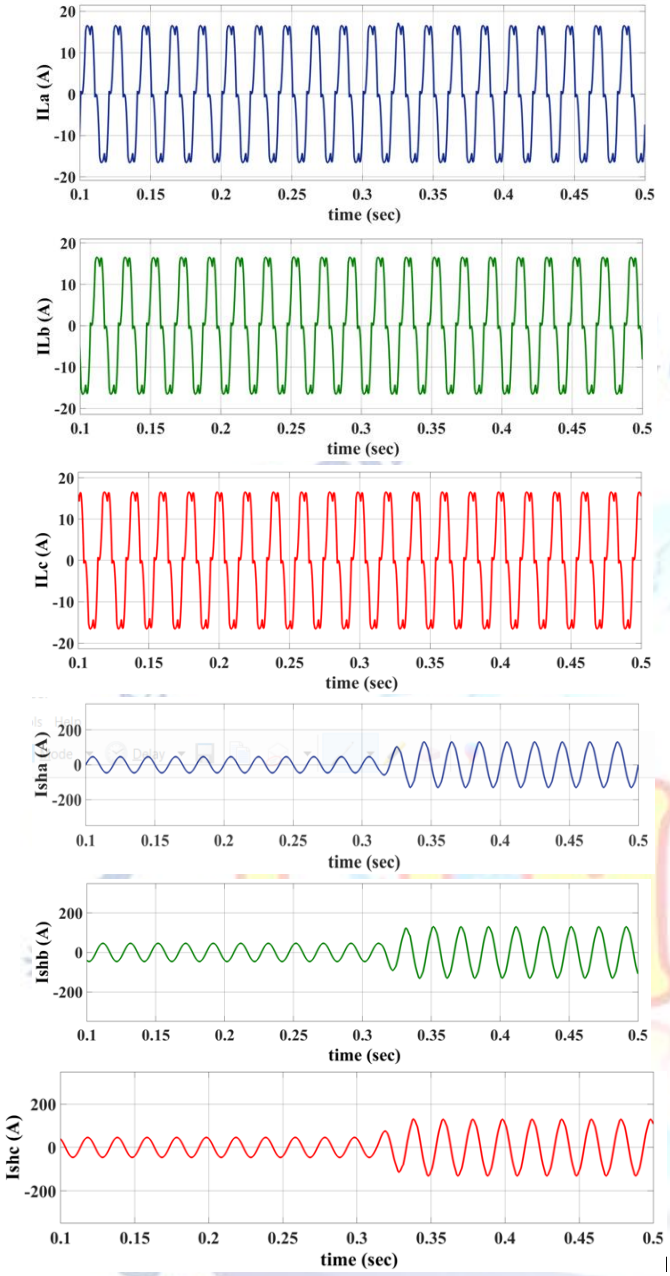

Fig. 12. Performance PV-UPQC at varying irradiation condition.

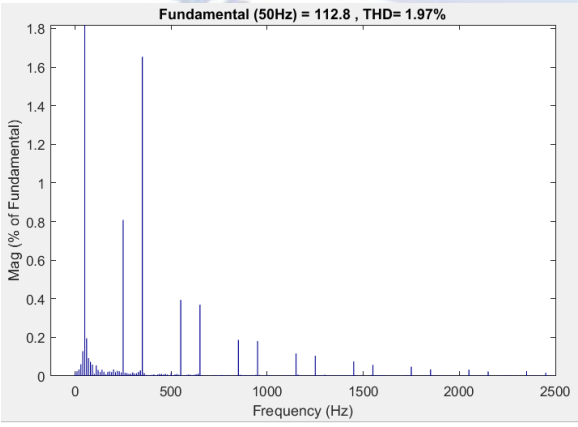

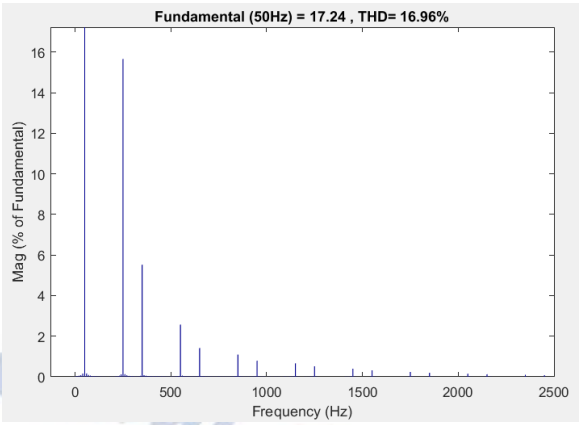

Fig. 13. THD for Grid current and load current

7. CONCLUSION

The complexity of power quality issues such harmonics, voltage surges and dips, and voltage interruptions under an unbalanced and distorted voltage grid has prompted study into the design and installation of three-phase UPQC. The UPQC provides the network with active power capacity when paired with (energy) ESS and PV. The capacity to generate and use active electricity from PV is the primary advantage of integrating ESS with UPQC. Because of this dependency on the external environment, renewable energy sources are not always reliable; this is where an ESS comes in. To sum up, ESS and PV combined with UPQC are seen as a potentially beneficial solution in distributed generation for improving the power quality of the modern distribution system. Due to the consistent power output of the PV-ESS system, there will be no fluctuations in the DC-link voltage. As a result, the algorithm utilised to control the DC voltage might become simpler. Different lighting conditions, voltage fluctuations, and asymmetrical loads are used to test the system's dependability. In circumstances of load imbalance, MAF has made d-q control more effective. PV-UPQC, which combines distributed generation with power quality enhancement, may have significant implications for today's distribution system. Harmonic measurements of the grid current after using the suggested method proved conformity with the IEEE-519 standard. And last, it's important to stress that the suggested approach has the potential to boost efficiency across the grid power system as a whole.

Conflict of interest statement

Authors declare that they do not have any conflict of interest.

REFERENCES

[1]. M. J. E. Alam, K. M. Muttaqi, and D. Sutanto, "Mitigation of rooftop solar PV impacts and evening peak support by managing available capacity of distributed energy storage systems," IEEE Trans. Power Syst., vol. 28, no. 4, pp. 3874–3884, 2013.

[2]. L. Marin, A. Tarrasa, I. Candela, and P. Rodriguez, "Stability Analysis of a Grid-Connected VSC Controlled by SPC," 7th Int. IEEE Conf. Renew. Energy Res. Appl. ICRERA 2018, vol. 5, pp. 1209–1214, 2018.

[3]. V. Khadkikar, "Enhancing electric power quality using UPQC: A comprehensive overview," IEEE Trans. Power Electron., vol. 27, no.5, pp. 2284–2297, 2012.

[4]. D. De Yong, S. Bhowmik, and F. Magnago, ``Optimized complex power quality classifier using one vs. rest support vector machines," Energy Power Eng., vol. 9, no. 10, pp. 568_587, 2017.

[5]. A. Javadi, A. Hamadi, L. Woodward, and K. Al-Haddad, ``Experimental investigation on a hybrid series active power compensator to improve power quality of typical households," IEEE Trans. Ind. Electron., vol. 63, no. 8, pp. 4849_4859, Aug. 2016.

[6]. A. Javadi, L. Woodward, and K. Al-Haddad, ``Real-time implementation of a three-phase THSeAF based on a VSC and a PCR controller to improve the power quality of weak distribution systems," IEEE Trans. Power Electron., vol. 33, no. 3, pp. 2073_2082, Mar. 2018.

[7]. M. A. Mansor, M. M. Othman, I. Musirin, and S. Z. M. Noor, ``Dynamic voltage restorer (DVR) in a complex voltage disturbance compensation," Int. J. Power Electron. Drive Syst., vol. 10, no. 4, pp. 2222_2230, 2019.

[8]. A. Ghosh and G. Ledwich, ``Compensation of distribution system voltage using DVR," IEEE Trans. Power Del., vol. 17, no. 4, pp. 1030_1036, Oct. 2002.

[9]. S. Jothibasu and M. K. Mishra, ``A control scheme for storageless DVR based on characterization of voltage sags," IEEE Trans. Power Del., vol. 29, no. 5, pp. 2261_2269, Oct. 2014.

[10]. A. Farooqi, M. M. Othman, A. F. Abidin, S. I. Sulaiman, and M. A. M. Radzi, ``Mitigation of power quality problems using series active filter in a microgrid system," Int. J. Power Electron. Drive Syst., vol. 10, no. 4, pp. 2245_2253, 2019.

[11]. C. Kumar and M. K. Mishra, ``Operation and control of an improved performance interactive DSTATCOM," IEEE Trans. Ind. Electron., vol. 62, no. 10, pp. 6024_6034, Oct. 2015.

[12]. Y. Hoon, M. M. Radzi, M. Hassan, and N. Mailah, ``Control algorithms of shunt active power filter for harmonics mitigation: A review," Energies, vol. 10, no. 12, p. 2038, Dec. 2017.

[13]. L. B. G. Campanhol, S. A. O. da Silva, and A. Goedtel, ``Application of shunt active power filter for harmonic reduction and reactive power compensation in three-phase four-wire systems," IET Power Electron., vol. 7, no. 11, pp. 2825_2836, Nov. 2014.

[14]. Y. Hoon, M. A. M. Radzi, M. K. Hassan, and N. F. Mailah, ``Operation of three-level inverter-based shunt active power filter under nonideal grid voltage conditions with dual fundamental component extraction," IEEE Trans. Power Electron., vol. 33, no. 9, pp. 7558-7570, Sep. 2018.

[15]. E. Hossain, M. R. Tur, S. Padmanaban, S. Ay, and I. Khan, ``Analysis and mitigation of power quality issues in distributed generation systems using custom power devices," IEEE Access, vol. 6, pp. 16816_16833, 2018.

[16]. H. Fujita and H. Akagi, ``The unified power quality conditioner: The integration of series- and shunt-active filters," IEEE Trans. Power Electron., vol. 13, no. 2, pp. 315-322, Mar. 1998.

[17]. S. K. Khadem, M. Basu, and M. F. Conlon, ``Intelligent islanding and seamless reconnection technique for microgrid with UPQC," IEEE J. Emerg. Sel. Topics Power Electron., vol. 3, no. 2, pp. 483-492, Jun. 2015.

[18]. J. M. Guerrero, P. C. Loh, T.-L. Lee, and M. Chandorkar, ``Advanced control architectures for intelligent microgrids Part II: Power quality, energy storage, andAC/DC microgrids," IEEE Trans. Ind. Electron., vol. 60, no. 4, pp. 1263_1270, Apr. 2013.

[19]. B. Han, B. Bae, H. Kim, and S. Baek, ``Combined operation of unified power-quality conditioner with distributed generation," IEEE Trans. Power Del., vol. 21, no. 1, pp. 330_338, Jan. 2006.

[20]. K. Hasan, M. M. Othman, N. F. A. Rahman, M. A. Hannan, and I. Musirin, ``Signi_cant implication of uni_ed power quality conditioner in power quality problems mitigation," Int. J. Power Electron. Drive Syst., vol. 10, no. 4, p. 2231, Dec. 2019.

[21]. C. K. Sundarabalan, Y. Puttagunta, and V. Vignesh, ``Fuel cell integrated unified power quality conditioner for voltage and current reparation in four-wire distribution grid," IET Smart Grid, vol. 2, no. 1, pp. 60_68, Mar. 2019.

[22]. S. Devassy and B. Singh, ``Design and performance analysis of three- phase solar PV integrated UPQC," IEEE Trans. Ind. Appl., vol. 54, no. 1, pp. 73_81, Jan. 2018.

[23]. L. B. G. Campanhol, S. A. O. da Silva, A. A. de Oliveira, and V. D. Bacon, ``Power flow and stability analyses of a multifunctional distributed generation system integrating a photovoltaic system with unified power quality conditioner," IEEE Trans. Power Electron., vol. 34, no. 7, pp. 6241_6256, Jul. 2019.

[24]. A. M. Gee, F. Robinson, and W. Yuan, ``A superconducting magnetic energy storage-emulator/battery supported dynamic voltage restorer," IEEE Trans. Energy Convers., vol. 32, no. 1, pp. 55_64, Mar. 2017.

[25]. W. U. Tareen and S. Mekhilef, ``Transformer-less 3P3W SAPF (three- phase three-wire shunt active power filter) with line-interactive UPS (uninterruptible power supply) and battery energy storage stage," Energy, vol. 109, pp. 525_536, Aug. 2016.

[26]. S. K. Kollimalla, M. K. Mishra, and N. L. Narasamma, ``Design and analysis of novel control strategy for battery and supercapacitor storage system," IEEE Trans. Sustain. Energy, vol. 5, no. 4, pp. 1137_1144, Oct. 2014.

[27]. S. B. Karanki, N. Geddada, M. K. Mishra, and B. K. Kumar, ``A modfied three-phase four-wire UPQC topology with reduced DC-link voltage rating," IEEE Trans. Ind. Electron., vol. 60, no. 9, pp. 3555_3566, Sep. 2013.

[28]. A. Teke, L. Saribulut, and M. Tumay, ``A novel reference signal gen- eration method for power-quality improvement of uni_ed power-quality conditioner," IEEE Trans. Power Del., vol. 26, no. 4, pp. 2205_2214, Oct. 2011.

[29]. V. G. Kinhal, P. Agarwal, and H. O. Gupta, ``Performance investigation of neural-network-based uni_ed power-quality

conditioner," IEEE Trans. Power Del., vol. 26, no. 1, pp. 431_437, Jan. 2011.

[30]. B. Singh, A. Chandra, and K. A. Haddad, Power Quality: Problems and Mitigation Techniques. Hoboken, NJ, USA: Wiley, 2015.

[31]. B. Singh and J. Solanki, "A comparison of control algorithms for dstatcom," IEEE Trans. Ind. Electron., vol. 56, no. 7, pp. 2738–2745, Jul. 2009.

[32]. B. Singh, C. Jain, S. Goel, A. Chandra, and K. Al-Haddad, "A multifunctional grid-tied solar energy conversion system with ANF-based control approach," IEEE Trans. Ind. Appl., vol. 52, no. 5, pp. 3663–3672, Sep. 2016.

[33]. S. Golestan, M. Ramezani, J. M. Guerrero, and M. Monfared, "dq-frame cascaded delayed signal cancellation- based PLL: Analysis, design, and comparison with moving average filter-based PLL," IEEE Trans. Power Electron., vol. 30, no. 3, pp. 1618 1632, Mar. 2015.

[34]. R. Pea-Alzola, D. Campos-Gaona, P. F. Ksiazek, and M. Ordonez, "Dclink control filtering options for torque ripple reduction in low-power wind turbines," IEEE Trans. Power Electron., vol. 32, no. 6, pp. 4812–4826, Jun. 2017.

[35]. S. Golestan, M. Ramezani, J. M. Guerrero, F. D. Freijedo, and M. Monfared, "Moving average filter based phase-locked loops: Performance analysis and design guidelines," IEEE Trans. Power Electron., vol. 29, no. 6, pp. 2750–2763, Jun. 2014.

[36]. B. Subudhi and R. Pradhan, "A comparative study on maximum power point tracking techniques for photovoltaic power systems," IEEE Trans. Sustain. Energy, vol. 4, no. 1, pp. 89–98, Jan. 2013.

[37]. A. Sadigh and K. Smedley, "Review of voltage compensation methods in dynamic voltage restorer DVR," in Proc. IEEE Power Energy Soc. Gen. Meeting, Jul. 2012, pp. 1–8.

[38]. A. Rauf and V. Khadkikar, "An enhanced voltage sag compensation scheme for dynamic voltage restorer," IEEE Trans. Ind. Electron., vol. 62, no. 5, pp. 2683–2692, May 2015.